Biosensors and Bioelectronics 33 (2012) 152–157

Contents lists available at SciVerse ScienceDirect

Biosensors and Bioelectronics

journal homepage: www.elsevier.com/locate/bios

# Boron δ-doped (1 1 1) diamond solution gate field effect transistors

Robert Edgington[a], A. Rahim Ruslinda[b], Syunsuke Sato[b], Yuichiro Ishiyama[b], Kyosuke Tsuge[b], Tasuku Ono[b], Hiroshi Kawarada[b], Richard B. Jackman[a,*]

[a] London Centre for Nanotechnology, and Department of Electronic and Electrical Engineering, University College London, 17-19 Gordon Street, London, WC1H 0AH, UK
[b] Department of Electronic and Photonic Systems, Waseda University, Okubo 3-4-1, Shinjuku, Tokyo 169-8555, Japan

ARTICLE INFO

*Article history:*
Received 11 November 2011
Received in revised form
22 December 2011
Accepted 25 December 2011
Available online 8 January 2012

*Keywords:*
Diamond
Delta-doping
Field-effect transistor
pH sensor
ISFET

ABSTRACT

A solution gate field effect transistor (SGFET) using an oxidised boron δ-doped channel on (1 1 1) diamond is presented for the first time. Employing an optimised plasma chemical vapour deposition (PECVD) recipe to deposit δ-layers, SGFETs show improved current–voltage (*I–V*) characteristics in comparison to previous similar devices fabricated on (1 0 0) and polycrystalline diamond, where the device is shown to operate in the enhancement mode of operation, achieving channel pinch-off and drain-source current saturation within the electrochemical window of diamond. A maximum gain and transconductance of 3 and 200 μS/mm are extracted, showing comparable figures of merit to hydrogen-based SGFET. The oxidised device shows a site-binding model pH sensitivity of 36 mV/pH, displaying fast temporal responses. Considering the biocompatibility of diamond towards cells, the device's highly mutable transistor characteristics, pH sensitivity and stability against anodic oxidation common to hydrogen terminated diamond SGFET, oxidised boron δ-doped diamond SGFETs show promise for the recording of action potentials from electrogenic cells.



## 1. Introduction

The hydrogenated surface conductive channel (H-SCC) of diamond is a unique material region for ion sensitive field effect transistors (ISFETs). Its strong polarisability (Pleskov, 2002), embodied by its wide band gap, strong resistance to corrosion and large surface dipole barrier mean that, unlike silicon based ISFETs, gate oxide passivation layers are not required to avoid large faradaic leakage currents and device degradation. Instead the H-SCC can operate as a solution gate field effect transistor (SGFET) with its gate and conductive channel directly exposed to an analyte solution (Kawarada et al., 2001), yet does not suffer from reduced transconductance due to diminished gate potentials across the gate oxide layer or device deterioration due to trapped ions permeating into the gate oxide layer. Appropriately, H-SCC SGFETs display increased sensitivity, exhibiting large responses to pH changes near the theoretical Nernst limit of 59 mV/pH (Garrido et al., 2005; Rezek et al., 2007); have saturated output characteristics within the electrochemical potential window of water and can be used to perform sensitive potentiometric molecular biosensing (Ruslinda et al., 2010) or record electrogenic activity in cells (Dankerl et al., 2009).

Whilst H-SCC SGFETs demonstrate excellent sensitivity and device characteristics, the H-SCC channel has proved unsuitable for long-term application due to its instabilities, including a tendency to undergo anodic oxidation during operation (Rezek et al., 2006), a dependence on external adsorbates to form its conductive channel (Ristein, 2006), differing fabrication methods resulting in H-SCCs with differing electrical properties (Nebel et al., 2006) and varying pH responses (Kawarada et al., 2001; Garrido et al., 2005; Nebel et al., 2006; Rezek et al., 2006; Song et al., 2006; Dankerl et al., 2008; Sasaki and Kawarada, 2010). Instead, a more robust substitutional doping method is needed; however, few elements are suitable for substitutional doping in diamond. The elements which are suitable (notably phosphorous, nitrogen and boron) have large thermal activation energies (Borst and Weis, 1996; Kalish, 1999) and, as a result, only a small fraction of these impurities are ionised to give free charge carriers at room temperature. Boron – diamond's lowest activation energy dopant – still has an activation energy of 0.37 eV at low doping concentrations of $<10^{17}$ cm$^{-3}$, and conductive channels from such a material result in thermally dependent, low transconductance channels that make poor FETs. To decrease the activation energy of boron in diamond one can increase the doping concentration. This continues to a point until approximately $3 \times 10^{20}$ cm$^{-3}$ where a metallic impurity band forms and the activation energy of the boron dopants tends to zero (Bustarret et al., 2008). However, as the carrier activation energy decreases so does the carrier mobility due to increased impurity scattering (Borst and Weis, 1996) and the onset of a hopping-like conduction

* Corresponding author. Tel.: +44 2076791381; fax: +44 2076790595.
*E-mail address:* r.jackman@ucl.ac.uk (R.B. Jackman).

0956-5663/$ – see front matter © 2011 Elsevier B.V. All rights reserved.
doi:10.1016/j.bios.2011.12.044

mechanism. The resultant material is one with inadequate mobilities (0.1–2 $cm^2/V\,s$ (Borst and Weis, 1996)) for responsive FET operation with sheet carrier densities typically in excess ($>4 \times 10^{13}\,cm^{-2}$) (Denisenko and Kohn, 2005) of what is controllable by a field effect transistor (FET).

δ-Doping, a technique borrowed from the III–V semiconductor community (Schubert and Ploog, 1985), could remedy the excessive sheet carrier density and low carrier mobility associated with metallic boron doped channels. In theory, δ-doping works by reducing the thickness of a heavily doped layer to a thickness significantly smaller than the de Broglie wavelength of holes in diamond (10 nm, Nebel et al., 2006), so that the charge distribution of the carriers can form a V-shaped potential well within which a 2D hole gas forms that extends into the higher mobility surrounding intrinsic diamond (Schubert et al., 1986). The simple reduction of channel thickness also reduces the sheet carrier density of the channel to FET gate-mutable levels whilst the delocalisation of carriers into the higher mobility intrinsic diamond lends the channel a higher carrier mobility (Fiori et al., 2010). δ-Doped diamond SGFETs could improve on H-SCC SGFETs by the possibility of high channel mobilities and its surface functionalisation being less constrained by not having to maintain its hydrogenation, allowing for more versatile and tailored surface functionalisations for applications such as molecular biosensing, specific chemical sensing or electrogenic cell recording.

In practice, depositing heavily-doped abrupt δ-layers is not a simple task and few mobility enhancements have been reported in the literature (El-Hajj et al., 2008). Unlike the III–V semiconductor industry, where molecular beam epitaxy can be used to precisely deposit dopant monolayers, the less controllable method of plasma enhanced chemical vapour deposition (PECVD) must be used for diamond deposition. Moreover, additional to the channel specifications required for the formation of a 2D gas, SGFETs demand further specifications on their conductive channel if they are to display saturated transistor characteristics within the electrochemical potential window of diamond and operate in the preferred enhancement mode of operation ($V_T < 0$, "always off"). Considering a p-type enhancement planar-doped MESFET regime of operation, δ-layers of approximately 1 nm thickness with $10^{20}\,cm^{-3}$ boron concentration are required.

To date, despite 1 nm metallic δ-layers using the (1 0 0) diamond plane being reported in the literature (El-Hajj et al., 2008), subsequent fabrications of SGFET have resulted in always-on, low gain and transconductance devices with unsaturated linear current–voltage (*I–V*) characteristics (Denisenko et al., 2007). As an alternative, herein the (1 1 1) diamond plane as a substrate for δ-growth for SGFET application is investigated. Firstly, with respect to growing abrupt heavily-doped δ-layers, the (1 1 1) diamond plane could be favourable due to its eight times higher boron incorporation density than the (1 0 0) plane (Ushizawa et al., 1998) and its superior ability at sustaining high doping levels at low film thicknesses (Kitagoh et al., 2010). The authors have already demonstrated that (1 1 1) diamond can support higher doping densities for a given mobility value than diamond (1 0 0) (Ye et al., 2008), and enhanced mobilities along with near-ideal sheet carrier densities are reported for δ-doped (1 1 1) diamond layers (Edgington et al., 2012). Additional to possible electrical advantages, the use of the oxygenated (1 1 1) diamond plane could be of principal advantage in improving SGFET I-V characteristics and pH sensitivity. Oxygen moieties on the (1 0 0) diamond surface are known to have a high density of surface states that readily pin the surface Fermi level and permanently deplete (1 0 0) δ-layers (Denisenko et al., 2008). Experimentally, in order to compensate such pinning, thicker δ-layers are typically fabricated leading to always-on, linear regime SGFETs. In contrast, it has been suggested (Ri et al., 2006) that the oxygenated (1 1 1) diamond surface is not pinned by surface states, which could allow for thinner δ-layers with lower threshold voltages, saturated output characteristics and enhanced transconductance. With respect to enhancing pH sensitivity, (1 1 1) diamond is preferentially oxidised by hydroxyl groups (de Theije et al., 2001) and the density of these amphoteric oxygen moieties are thought to be responsible for determining the pH sensitivity of ISFETs in the site binding model (Yates et al., 1974; Garrido et al., 2005). The fabrication and *I–V* characterisation of uncapped oxidised boron δ-doped (1 1 1) diamond SGFETs is presented, and their *I–V* characteristics and response to different pH solutions is investigated.

## 2. Materials and methods

### 2.1. δ-Layer deposition

To fabricate SGFET, (1 1 1) δ-doped diamond layers were deposited on 2 mm × 2 mm (1 1 1) diamond substrates (Suitomo Electric Ltd., Japan). Intrinsic undoped diamond epilayers of ca. 600 nm thickness and ca. 2 nm average roughness (as determined by atomic force microscopy, AFM) were deposited using PECVD in ASTeX AX2050 or Seki Technotron Corp AX5010 reactors as described in Table A1. Heavily-doped boron layers were deposited in a NIRIM-type PECVD reactor using trimethylboron (TMB) as a boron source also as described in Table A1. Two PECVD recipes were used: δ1; a preliminary metallic boron-doped diamond recipe (Kitagoh et al., 2010) and δ2; an optimised PECVD recipe for δ-layer growth as detailed in Edgington et al. (2012). Both recipes were designed to give ca. 1 nm δ-layers with ca. $10^{20}\,cm^{-3}$ boron concentration. Equivalent δ-layers have sheet carrier densities of ca. $10^{13}\,cm^{-2}$ and mobilities of ca. 10 $cm^2/V\,s$, as measured by AC Hall effect, and boron densities of ca. $10^{20}\,cm^{-3}$ and thicknesses of ca. 1–2 nm, as described in detail in Edgington et al. (2012). Grown δ-doped layers had average roughness of ca. 2.5 nm. Plasmas were extinguished 1 min after $CH_4$ flow was stopped and all samples were cooled for 20 min in 50 Torr, 400 sccm $H_2$ ambients. Prior to PECVD all reactors were evacuated to at least $5 \times 10^{-6}$ Torr. Samples were left uncapped, i.e. without further deposition of capping intrinsic diamond.

### 2.2. SGFET fabrication

Following δ-deposition, titanium and gold (20 nm and 100 nm respectively) source and drain contacts were deposited on oxygenated uncapped δ-layers using an Edwards A500 Electron Beam Evaporator, and patterned using lift-off photolithography using AZ 5214 E image reversal photoresist. The contacts were positioned to give a 2 mm channel width and 80 μm channel length. Contacts were annealed at 700 K in a hydrogen atmosphere (20 Torr, 100 sccm, 30 min) (Jingu et al., 2010) to impart ohmic properties. Samples were oxygen terminated before and after contact formation with a UV photochemical treatment (Sakai et al., 2003; Jingu et al., 2010) in the presence of ozone for 3 h to suppress hydrogen surface conductivity and provide hydroxyl sites for pH sensitivity. Passivation of source and drain contacts was achieved using 2 μm SU-8 2002 photoresist. Three gaps were patterned into the passivation to form: (1) a gate region (2 mm width, 60 μm length), (2) source and (3) drain back contacts (Fig. 1(a)). Samples were fixed onto glass slides with epoxy, and gold wires were bound with silver paste to the source and drain contacts (Fig. 1(b)). Gold wires were then bound to insulated wires with CW2400 Araldite conductive epoxy and all exposed conductive regions (except the gate) were insulated with Araldite 2014 epoxy (Fig. 1(c)). A dummy sample was also fabricated without boron doping, but otherwise identical processing, which resulted in highly resistive channels (>10 GΩ).

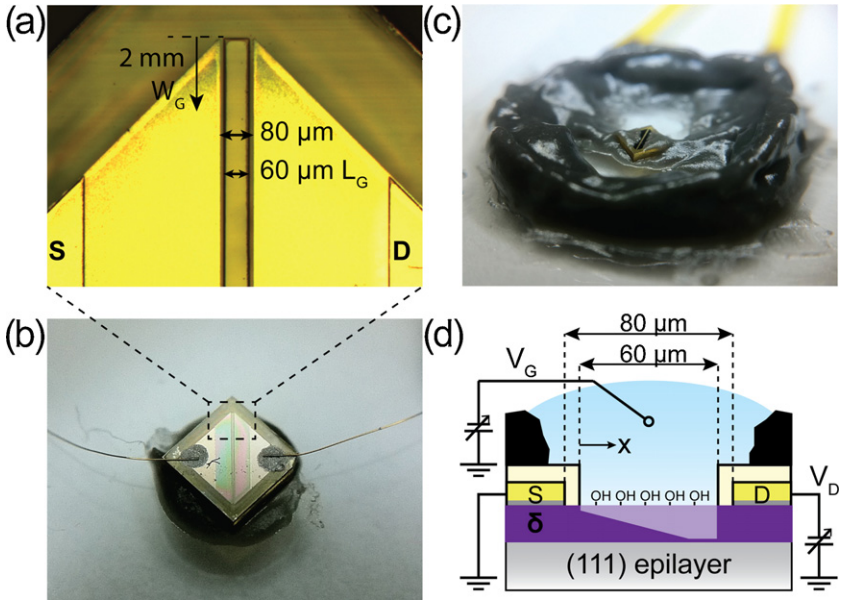


**Fig. 1.** (a) Micrograph of SGFET source, gate and drain showing passivation openings. (b) Macro photograph of wire bonded device prior to encapsulation. Sample is 2 mm × 2 mm. (c) Epoxy encapsulated SGFET. (d) Experimental setup of SGFET using a MESFET analogy, depicting the channel depleted in the saturation regime.

### 2.3. *I–V characterisation and pH testing*

*I–V* characterisation of SGFET was performed using two Keithley 2400 source and measurement units interfaced with a custom Labview program, using an Ag/AgCl reference electrode in the experimental setup depicted in Fig. 1(d) that applies gate potential uniformly along the whole channel length. Measurements were recorded in 1 mM PBS or Carmody Universal Buffer (Carmody, 1961) solution (0.2 M boric acid, 0.05 M citric acid and 0.1 M trisodium phosphate as a pH adjuster) varied between pH 2 and 12 pH was measured using a calibrated pH meter (HS-205C TOA Electronics Ltd., Tokyo, Japan). pH transfer characteristics were taken after stabilisation with a fixed drain-source voltage of $-0.6\,V_{DS}$. Real time pH recordings were performed at $-0.9\,V_{GS}$, $-0.6\,V_{DS}$. SGFETs were rinsed before and after measurements in DI water and dried by $N_2$ gun, except in real time pH measurements where tri-sodium phosphate solution was added in calculated aliquots to increase the pH by 1 pH unit per addition, or as stated.

## 3. Results and discussion

### 3.1. *δ1 SGFET I–V characteristics*

Fig. 2(a) and (b) shows the output and transfer characteristics of the non-optimised SGFET using PECVD recipe δ1. Output characteristics between 0 and $-0.6\,V_{DS}$ and +0.6 and $-0.6\,V_{GS}$ show the device to operate in the linear regime with no discernable channel pinch-off within the electrochemical potential window of diamond. A low transconductance ($g_m$) and maximum gain ($g_m/G$, where $G$ is conductance) of 20 µS/mm and 0.35 (at $-0.6\,V_{GS}$, $-0.3\,V_{DS}$) respectively are measured. Positive gate voltages serve to deplete the channel, as expected for a p-type conductive channel, however the channel could not be depleted within the electrochemical window of diamond, resulting in an always-on depletion mode device. Extrapolating transfer curves (Fig. 2(b)) an estimated threshold voltage ($V_T$) of 2 V is obtained. Using a non-optimised PECVD recipe, the *I–V* characteristics of δ1 SGFET result in a linear depletion mode device with similar output characteristics to previous SGFET fabricated on (1 0 0) diamond (Denisenko et al., 2007). Whilst δ1 SGFET has a different gate length to that SGFET, both show similar transconductances of 20 µS/mm at $-0.6\,V_{DS}$. However, δ1 SGFET shows a higher gain of 0.35, which is irrespective of device dimensions, in comparison to the 0.16 gain extracted from the aforementioned device (Denisenko et al., 2007).

### 3.2. *δ2 SGFET I–V characteristics*

Following *I–V* characterisation of δ1 SGFET, δ2 SGFET was investigated. Employing the optimised PECVD recipe δ2, the *I–V* characteristics of δ2 SGFET show significantly improved output and transfer characteristics, critically operating in the favoured saturation regime and enhancement mode of operation. Output characteristics between 0 and $-0.6\,V_{DS}$ and 0.2 to $-1\,V_{GS}$ show the device to achieve channel pinch-off within the electrochemical window of diamond (Fig. 3(a)), showing always-off characteristics in the enhancement mode of operation. The transfer curves of the SGFET show the current output not to be subject to variations in drain-source voltage when greater than approximately $-0.5\,V_{DS}$. Taking the transfer curve gradient in the saturation regime, a

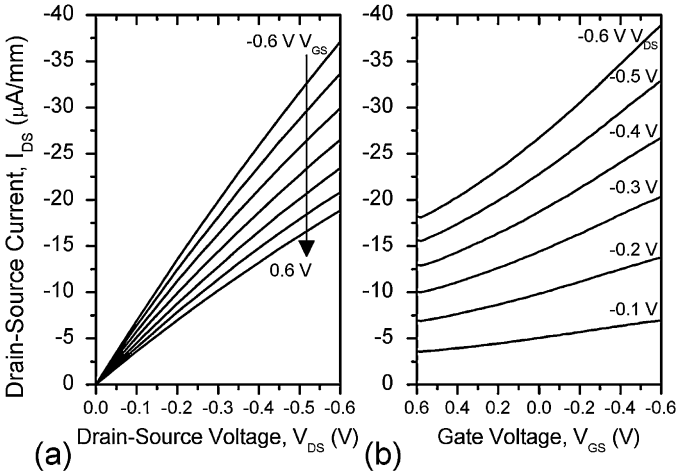


**Fig. 2.** (a) Output characteristics and (b) transfer characteristics of δ1 SGFET in 1 mM PBS. $Gain_{max}$: 0.35. $g_m$: 20 µS/mm $V_T$ ca. $2\,V_{GS}$.

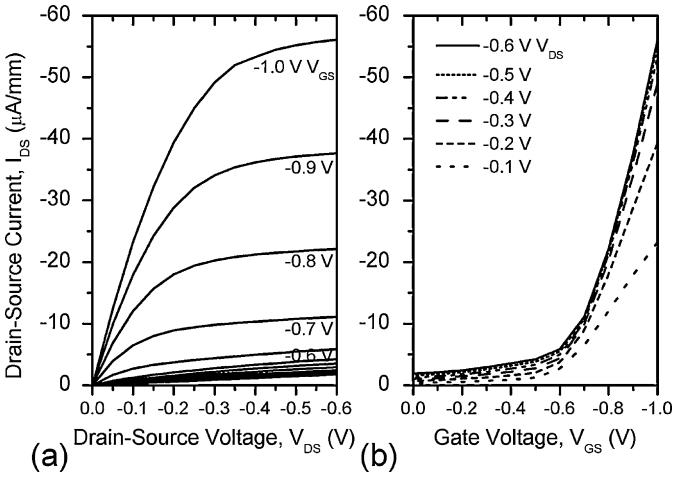


**Fig. 3.** (a) Output characteristics and (b) transfer characteristics of δ2 SGFET in 1 mM PBS. $Gain_{max}$: 3. $g_m$: 200 μS/mm. $V_T$ −0.6 $V_{GS}$.

transconductance of 200 μS/mm and a maximum gain of 3.0 (at −0.8 $V_{GS}$, −0.6 $V_{DS}$) are obtained.

In comparison to hydrogen-based SGFETs, the measured transconductance of 50 μS/mm and gain of 1.1 at −0.2 $V_{DS}$ and −0.7 $V_{GS}$ for δ2 SGFET are comparable to the 80 μS/mm and 1.6 gain reported (Rezek et al., 2007) at similar operating conditions for purely hydrogenated SGFET; significantly larger than the 0.22 μS/mm and 0.01 gain reported (Garrido et al., 2005) for a partially oxidised hydrogenated SGFET and similar to the 15 μS/mm and 1.0 gain as calculated from data reported (Sasaki and Kawarada, 2010) for another partially oxidised hydrogenated SGFET.

As well as improved transconductance and gain, δ2 SGFET shows the preferable enhancement mode operation with a $V_T$ of ∼ −0.6 $V_{GS}$, which is indicative of a downward positive surface barrier potential being present on the oxygenated device surface. Adapting a planar doped FET model (Kwok, 1995) for a uniformly doped p-type surface channel (δ-layer) with a gate reference electrode, the origin of a negative $V_T$ can be investigated by examination of the terms of $V_T$, which can be expressed as follows:

$$-V_T = E_{ref} - \psi_0 + \chi^{sol} - \frac{\phi_\delta}{q} - V_p - \frac{qN_A a^2}{2\varepsilon_s} \quad (1)$$

where the first four terms constitute the equivalent of a Schottky barrier between the diamond and reference electrode (see Shinwari et al., 2007 for further details) and are constant upon pH change, except for $\Psi_0$ and $\chi^{sol}$, the electrolyte interface potential and the surface dipole potential of the electrolyte, however changes in $\chi^{sol}$ are negligible in comparison to $\Psi_0$. Oxide and interface charges are not included due to the lack of a gate oxide layer. $V_p$ is the Fermi level of bulk diamond away from the doped layer relative to the valence band and the final term is the pinch-off voltage of the channel, $V_{PO}$, wherein $a$ is δ-layer thickness, $N_A$ is acceptor concentration ($cm^{-3}$), $q$ is the elementary charge and $\varepsilon_s$ is permittivity. From Eq. (1) it can be seen that the measured negative $V_T$ can only arise from the Schottky barrier terms because the other terms are positive for p-type channels. Using estimated δ-layer parameters (1 nm δ, $N_A$ $10^{20}$ $cm^{-3}$, $\varepsilon_s$ 5.5 and $V_p$ 0.37 eV (from unintentional boron doping adjacent to the δ)) and the measured $V_T$ of −0.6 V, this gives a Schottky barrier of approximately 1.1 eV, which is comparable to typical values for oxygenated diamond surface barriers (Pietzka et al., 2010). Such a positive barrier could result from either an unpinned oxygenated diamond surface equilibrating with a higher chemical potential PBS solution, or alternatively from Fermi level pinning and downward band bending from dense oxygen states on the δ-layer surface. Since the observed pH sensitivity of the

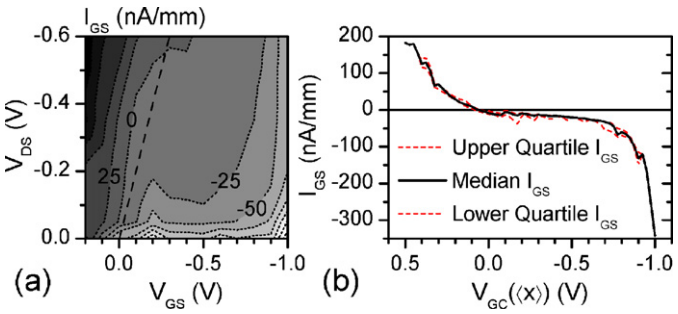


**Fig. 4.** (a) Gate-source current leakage ($I_{GS}$) contour map with respect to $V_{DS}$ and $V_{GS}$, with shaded increments of 25 nA. The long-dash line represents average zero gate-channel potential ($V_{GC}$). (b) Median $I_{GS}$ vs. $V_{GC}$ with upper and lower quartile error envelopes.

device is indicative of an unpinned band edge (see Section 3.3), the former explanation seems most likely, i.e. an unpinned oxidised (1 1 1) surface, but with an additional low density of surface states due to an imperfectly smooth gate surface (2.5 nm $R_a$), that introduces binding sites favoured by more complicated, state-including oxygen moiety functionalisations (Denisenko et al., 2008).

Gate leakage current analysis (Fig. 4(a)) shows that, in the operational range of the device, gate leakages are less than 25 nA with a gate resistance of 12 MΩ. Negative gate-channel voltages ($V_{GC}(x) = V_{GS} - V_{DS}(x)$) in excess of −0.8 $V_{GC}$ and positive voltages greater than approximately 0 $V_{GC}$ result in exponential faradaic current generation (Fig. 4(b)). In terms of device symmetry, gate leakage passes zero near the point of average zero gate-channel potential ($V_{GC}(\langle x \rangle) = (V_{GS} - V_{DS}/2)$, Fig. 4(a) and (b)), which is indicative of a device with little leakage bias to the source or drain end of the gate.

### 3.3. δ2 SGFET pH sensitivity

The pH sensitivity of δ2 SGFET was then investigated using Carmody Universal Buffer between pH 2 and pH 12. Transfer characteristics of δ2 SGFET for different pH-adjusted solutions are displayed in Fig. 5(a), wherein low pH gives a low $I_{DS}$ output with a more negative value of $V_T$, and vice versa. The pH sensitivity of δ2 SGFET behaves as expected for a p-type oxidised SGFET following the site-binding model (Yates et al., 1974; Bousse et al., 1983; Nebel et al., 2006) of pH sensitivity: pH dependent protonation and deprotonation of amphoteric hydroxyl sites on the device gate – as determined by chemical equilibration with the bulk electrolyte (low pH: C—$OH_2^+$, neutral: C—OH high pH: $CO^-$) – results in the δ-channel charge density (and therefore $I_{DS}$) being modulated by the built up surface potential in order to maintain charge neutrality

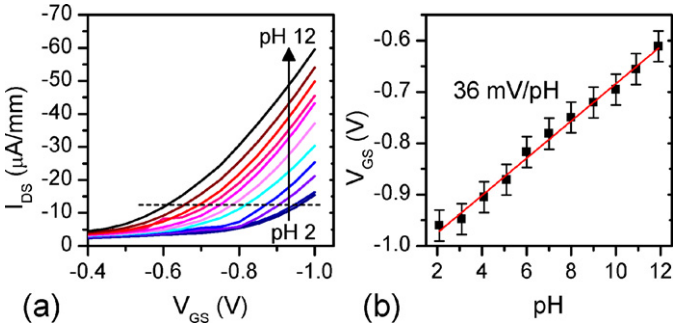


**Fig. 5.** (a) Transfer characteristics ($V_{DS}$ = −0.6 V) for δ2 SGFET at different pH. (b) $V_{GS}$ shift vs. pH for $I_{DS}$ of −12.5 μA. pH is varied from pH 2 to 12 using Carmody Universal Buffer. $V_{GS}$ error bars correspond to a generous maximum variance (±0.03 V) of gate voltage drift between measurements, and pH error bars of ±0.1 pH are too small to be shown.

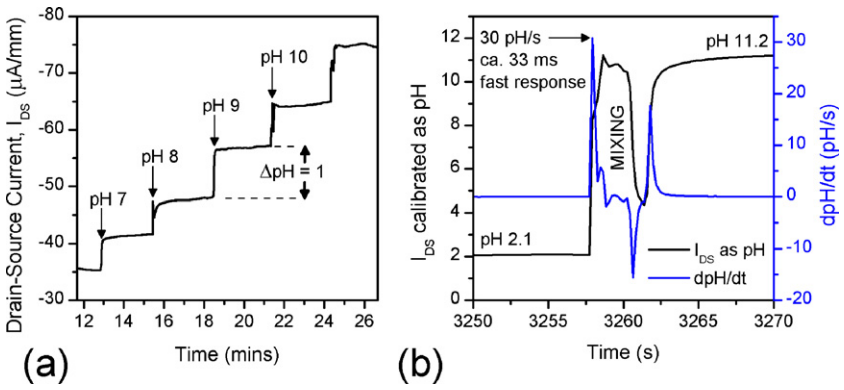


**Fig. 6.** (a) pH titration of Carmody buffer in pH 1 increments via the addition of appropriate aliquots of tri-sodium phosphate. (b) A large addition of tri-sodium phosphate is made to give a pH 2.1 to pH 11.2 step, from which an upper limit of the fast response of 33 ms is estimated. Erratic data during the step is from solution mixing.

throughout the device. For example, in the case of high pH, where deprotonation of amphoteric sites occurs, the negative charge next to the δ-channel removes depletion increasing the hole current of the channel (Fig. 5(a)). It should be noted that as well as the accumulated surface charges in the inner Helmholtz plane (IHP), charge neutrality must be achieved for the counter charges in the outer Helmholtz plane (OHP), Stern and diffuse layer, which allows sensitivity to larger ion concentrations such as $K^+$ and $Na^+$, which cannot permeate (without specific adsorption) into the IHP.

In terms of device *I–V* characteristics, the effect of pH and resultant accumulated surface charge manifests itself in a change in $V_T$ via the electrolyte surface potential, $\psi_0$, a term contained in the expression for $V_T$ (Eq. (1)), as can be seen in Fig. 5(a) as a negative shift of $V_T$ with increasing pH. The shift in the surface potential with respect to the bulk pH, $pH_B$, can be described as in Eq. (2) (van Hal et al., 1996), where the maximum $V_T$ shift possible is the Nernstian response of ca. 59 mV/pH, $\alpha$ is the sensitivity parameter ($\alpha \leq 1$) associated with the oxide layer, $C_{DL}$ is the double-layer capacitance and $\beta_{int}$ is the intrinsic buffer capacity of the surface defined by the density of surface binding sites charged per unit surface pH ($pH_s$) change.

$$\frac{d\psi_0}{dpH_B} = \alpha.2303\frac{k_BT}{q_a} = -\alpha.59\,\text{mV} \tag{2}$$

where

$$\alpha = \left|\frac{2.303k_BT}{q_a^2}\frac{C_{DL}}{\beta_{int}} + 1\right|^{-1} \tag{3}$$

Using a fixed current of −12.5 μA/mm, the gate voltage shift (and thereby $\Psi_0$) with respect to pH has been extracted giving a pH sensitivity (as determined by linear fit) of $d\Psi_0/dpH_B$ = 36 mV/pH (Fig. 5(b)). Whilst there is slight non-linearity in the pH response and a slight increase in $g_m$ for a fixed $I_{DS}$ with increasing pH (where $g_m \propto \mu$), which could possibly be ascribed to non-linear changes of mobility vs. carrier density associated with sloped conduction bands (Rezek et al., 2006) (such as in a delocalised δ-layer), the drift error in measurements precludes this observation and under these operating parameters the device offers a near-linear response to pH change with similar transconductances for different pH solutions. The $d\Psi_0/dpH_B$ of 36 mV/pH measured for δ2 SGFET is smaller than anticipated considering the high density of amphoteric hydroxyl sites expected on the diamond surface and the large pH sensitivities reported on similar oxidised boron doped diamond SGFETs (Denisenko et al., 2007; Dipalo et al., 2008), which report sensitivities of 50 mV/pH near the Nernst limit of 59 mV/pH. Inspecting Eq. (3), the lower pH sensitivity could be ascribed to a large $C_{DL}$ and/or a low value for $\beta_{int}$, which can indicate a lower density of hydroxyl sites or small surface complex dissociation constants (van Hal et al., 1996). This simplified model could imply that the conductive channel could be actually a partially O-terminated H-SCC and not an oxidised δ-doped channel; however, the dummy SGFET, fabricated identically but without the boron-doping process step, has very resistive channels (>10 GΩ) that would not demonstrate such characteristics as presented here, which, in essence should mimic an H-SCC SGFET due to their similarities in sheet carrier density, mobility and band structure. Alternatively a partial pinning of the valence band edge from complicated oxygen moieties could be lowering the response of δ2 SGFET to pH change.

In order to investigate the time dependent response of the SGFET, pH titration experiments have been performed. Fig. 6(a) and (b) show δ2 SGFET to respond quickly to pH steps. Fig. 6(b) shows an estimate of the fast response time (the initial steep response (Bousse and Bergveld, 1984)), wherein $I_{DS}$ has been transformed into pH using pH meter calibration measurements. Taking the inverse of the maximum value of the derivative of pH vs. time over a large pH step (ca. 9 pH, Fig. 6(b)), an upper limit of the intrinsic fast response of ca. 33 ms is estimated. It should be noted this response time is largely reflective of the slower speed of pH titration rather than the intrinsic response of the SGFET, especially considering that, unlike other experiments (Bousse and Bergveld, 1984) which employ measures to reduce this effect, standard pipette mixing was used here. It is therefore expected that the device has a considerably lower intrinsic fast response in the millisecond range. Considering this, along with the highly biocompatible nature of oxidised diamond towards cells (Ariano et al., 2009a,b; Thalhammer et al., 2010) and the ability of oxidised SGFETs to sense $K^+$ and $Na^+$ ion concentration changes (Wrobel et al., 2005) that are in flux during electrogenic activity, oxidised δ-doped SGFET appear to be promising devices for the chronic recording of action potentials of electrogenic cells. Similarly, the high specific capacitance of diamond in comparison to other materials (Dankerl et al., 2009) could allow the stimulation of electrogenic cells on the same device. In terms of practical use, oxidative cleaning of the device should not degrade its *I–V* characteristics significantly because the device surface is already oxidised, making it suitable for long-term application.

## 4. Conclusions

SGFETs fabricated from oxidised boron δ-doped (1 1 1) diamond channels show improved *I–V* characteristics in comparison to equivalent devices built on (1 0 0) diamond and are comparable to H-SCC SGFETs. Following a PECVD recipe optimisation for δ-layer deposition on (1 1 1) diamond, subsequent SGFET fabrication results in a device exhibiting the desirable always-off enhancement mode of operation ($V_T$ −0.6 $V_{GS}$) with pinch-off and current

saturation being achieved within the electrochemical window of diamond. The SGFET shows good maximum gain and transconductance of 3 and 200 μS/mm respectively, with a moderate pH sensitivity of 36 mV/pH and fast temporal response to pH change. The immunity of the oxidised boron-doped diamond surface to anodic oxidation, its respectable *I–V* characteristics, pH sensitivity and high biocompatibility make oxidised boron δ-doped SGFETs promising devices for the chronic recording of action potentials from electrogenic cells and stable pH sensors.

## Acknowledgements

The UCL team acknowledge the UKs Engineering and Physical Sciences Research Council (EPSRC) for the award of a project to study δ-doped diamond structures (EP/H020055/1). Niall Tumilty and Rezal K. Ahmad of UCL are thanked for useful discussions relating to this work. One of us (RE) thanks the Japanese Society for the Promotion of Science (JSPS) for the award of a Research Fellowship to spend time at the University of Waseda. The work by one of the authors (HK) was supported by a Grant-in-Aid for Fundamental Research S (19106006) and A (23246069) from MEXT Japan.

## Appendix A. Supplementary data

Supplementary data associated with this article can be found, in the online version, at doi:10.1016/j.bios.2011.12.044.

## References

Ariano, P., Giudice, Lo, A., Marcantoni, A., Vittone, E., Carbone, E., Lovisolo, D., 2009a. Biosens. Bioelectron. 24, 2046–2050.
Ariano, P., Budnyk, O., Dalmazzo, S., Lovisolo, D., Manfredotti, C., Rivolo, P., Vittone, E., 2009b. Eur. Phys. J. E, 1–8.
Borst, T., Weis, O., 1996. Phys. Status Solidi (c) 154, 423–444.
Bousse, L., de Rooij, N., Bergveld, P., 1983. IEEE Trans. Electron. Devices 30, 1263–1270.
Bousse, L., Bergveld, P., 1984. Sens. Actuators 6, 65–78.
Bustarret, E., Achatz, P., Sacépé, B., Chapelier, C., Marcenat, C., Ortéga, L., Klein, T., 2008. Philos. Trans. R. Soc. Lond., Ser. A 366, 267–279.
Carmody, W.R., 1961. J. Chem. Educ. 38, 559.
Dankerl, M., Reitinger, A., Stutzmann, M., Garrido, J.A., 2008. Phys. Status Solidi (RRL) 2, 31–33.
Dankerl, M., Eick, S., Hofmann, B., Hauf, M., Ingebrandt, S., Offenhaeusser, A., Stutzmann, M., Garrido, J.A., 2009. Adv. Funct. Mater. 19, 2915–2923.
de Theije, F., Reedijk, M., Arsic, J., van Enckevort, W., Vlieg, E., 2001. Phys. Rev. B 64, 1–7.
Denisenko, A., Jamornmarn, G., El-Hajj, H., Kohn, E., 2007. Diamond Relat. Mater. 16, 905–910.
Denisenko, A., Pietzka, C., Romanyuk, A., El-Hajj, H., Kohn, E., 2008. J. Appl. Phys. 103, 1–8.
Denisenko, A., Kohn, E., 2005. Diamond Relat. Mater. 14, 491–498.
Dipalo, M., Pietzka, C., Denisenko, A., El-Hajj, H., Kohn, E., 2008. Diamond Relat. Mater. 17, 1241–1247.
Edgington, R., Sato, S., Ishiyama, Y., Morris, R., Jackman, R., Kawarada, H., 2012. J. Appl. Phys. 111 (3).
El-Hajj, H., Denisenko, A., Bergmaier, A., Dollinger, G., Kubovic, M., Kohn, E., 2008. Diamond Relat. Mater. 17, 409–414.
Fiori, A., Pernot, J., Gheeraert, E., Bustarret, E., 2010. Phys. Status Solidi A 207, 2084–2087.
Garrido, J.A., Härtl, A., Kuch, S., Stutzmann, M., Williams, O.A., Jackmann, R.B., 2005. Appl. Phys. 86, 073504.
Jingu, Y., Hirama, K., Kawarada, H.I, 2010. IEEE Trans. Electron. Devices 57, 966–972.
Kalish, R., 1999. Carbon, 781–785.
Kawarada, H., Araki, Y., Sakai, T., Ogawa, T., Umezawa, H., 2001. Phys. Status Solidi A 185, 79–83.
Kitagoh, S., Okada, R., Kawano, A., Watanabe, M., Takano, Y., Yamaguchi, T., Chikyow, T., Kawarada, H., 2010. Physica C 470, S610–S612.
Kwok, K., 1995. Complete Guide to Semiconductor Devices, 2nd ed. McGraw-Hill.
Nebel, C.E., Rezek, B., Shin, D., Watanabe, H., 2006. Phys. Status Solidi A 203, 3273–3298.
Pietzka, C., Denisenko, A., Romanyuk, A., Schaefer, P.J., Kibler, L.A., Scharpf, J., Kohn, E., 2010. Diamond Relat. Mater. 19, 213–216.
Pleskov, Y., 2002. Russ. J. Electrochem. 38, 1275–1291.
Rezek, B., Watanabe, H., Shin, D., Yamamoto, T., Nebel, C., 2006. Diamond Relat. Mater. 15, 673–677.
Rezek, B., Shin, D., Watanabe, H., Nebel, C.E., 2007. Sens. Actuators B: Chem. 122, 596–599.
Ri, S.-G., Nebel, C.E., Takeuchi, D., Rezek, B., Tokuda, N., Yamasaki, S., Okushi, H., 2006. Diamond Relat. Mater. 15, 692–697.
Ristein, J., 2006. J. Phys. D: Appl. Phys. 39, R71–R81.
Ruslinda, A.R., Tajima, S., Ishii, Y., Ishiyama, Y., Edgington, R., Kawarada, H., 2010. Biosens. Bioelectron. 26, 1599–1604.
Sakai, T., Song, K., Kanazawa, H., Nakamura, Y., Umezawa, H., Tachiki, M., Kawarada, H., 2003. Diamond Relat. Mater. 12, 1971–1975.
Sasaki, Y., Kawarada, H., 2010. J. Phys. D: Appl. Phys. 43, 1–8.
Schubert, E., Fischer, A., Ploog, K., 1986. IEEE Trans. Electron. Devices 33, 623–625.
Schubert, E., Ploog, K., 1985. Jpn. J. Appl. Phys. 24 (1), L608–L610.
Shinwari, M.W., Deen, M.J., Landheer, D., 2007. Microelectron. Reliab. 47, 2025–2057.
Song, K.-S., Nakamura, Y., Sasaki, Y., Degawa, M., Yang, J.-H., Kawarada, H., 2006. Anal. Chim. 573, 3–8.
Thalhammer, A., Edgington, R.J., Cingolani, L.A., Schoepfer, R., Jackman, R.B., 2010. Biomaterials 31, 2097–2104.
Ushizawa, K., Watanabe, K., Ando, T., Sakaguchi, I., Nishitani-Gamo, M., Sato, Y., Kanda, H., 1998. Diamond Relat. Mater. 7, 1719–1722.
van Hal, R.E.G., Eijkel, J.C.T., Bergveld, P., 1996. Adv. Colloid Interface Sci. 69, 31–62.
Wrobel, G., Seifert, R., Ingebrandt, S., Enderlein, J., Ecken, H., Baumann, A., Kaupp, U., Offenhausser, A., 2005. Biophys. J. 89, 3628–3638.
Yates, D.E., Levine, S., Healy, T.W., 1974. J. Chem. Soc. Faraday Trans. 1 (70), 1807–1818.
Ye, H., Tumilty, N., Bevilacqua, M., Curat, S., Nesládek, M., Bazin, B., Bergonzo, P., Jackman, R.B., 2008. J. Appl. Phys. 103, 054503.